Structural Safety and Reliability, Corotis et al. (eds), © 2001 Swets & Zeitlinger, ISBN 90 5809 197 X

Development of automated extraction method for building damage area based on maximum likelihood classifier

Hajime Mitomi, Fumio Yamazaki & Masashi Matsuoka
Earthquake Disaster Mitigation Research Center, RIKEN, Japan

Keywords: automated detection, building damage, maximum likelihood classifier, principal component analysis (PCA), real-time earthquake disaster management

ABSTRACT: Using some images taken from a helicopter after recent earthquakes, an automatic extraction method of the class of severely damaged buildings was examined by the maximum likelihood classifier with a multivariate normal distribution for the statistics of some training data in images. In the image processing, hue, saturation, brightness, edge intensity and variance of edge intensity were used for the extraction of information on damaged buildings, and the threshold value for each image did not have to be decided empirically such as in the method of Hasegawa et al. (2000b). The classification result was good for most of the classes used by this method. In particular, the class denoting collapsed buildings agreed well with the actual situation of building damage. Therefore, if we could set up some training data in each class, we would obtain favorite results for areas with building damage rapidly, and the application of this method to real-time earthquake disaster management can be expected.

1 INTRODUCTION

The 1995 Hyogoken-Nanbu (Kobe) Earthquake made us realize the importance of gathering damage information at an early stage of the recovery activity, without depending on information sent from within the stricken area. Several methods for gathering information on damage from the space and air above the stricken area are available, such as aerial television imagery, aerial photography and satellite imagery. Aerial television images and photographs, which have higher spatial resolution than satellite images, have been visually inspected (Hasegawa et al. 2000a, Ogawa & Yamazaki 2000). Although the severely damaged buildings could be visually inspected, a significant amount of time was required for visual interpretation. Therefore, Hasegawa et al. (2000b) carried out preliminary studies on automated damage detection based solely on the post event images taken by a high-definition television (HDTV) camera. The estimated distribution of building damage using the method proposed by them agreed relatively well with the ground truth data and the result of visual inspection of the HDTV images. Based on their study, Mitomi et al. (2000) applied the method to other images taken after the 1999 Kocaeli, Turkey and Chi-Chi, Taiwan earthquakes. We derived distributions close to the actual area of building damage, with the threshold values adjusted according to built environment for each image.

In the near future, satellite performance will be improved as high-resolution, hyper-spectrum and short recurrent period. Therefore, the Ministry of Construction in Japan is investigating techniques to detect damage due to earthquakes using high-resolution images simulated from aerial photographs (Nemoto et al. 2000). The project reveals the possibility of automated damage detection using not only aerial television images and photographs but also high-resolution satellite images. In this study, we developed the method for automated detection of building damage for application to real-time earthquake disaster management.

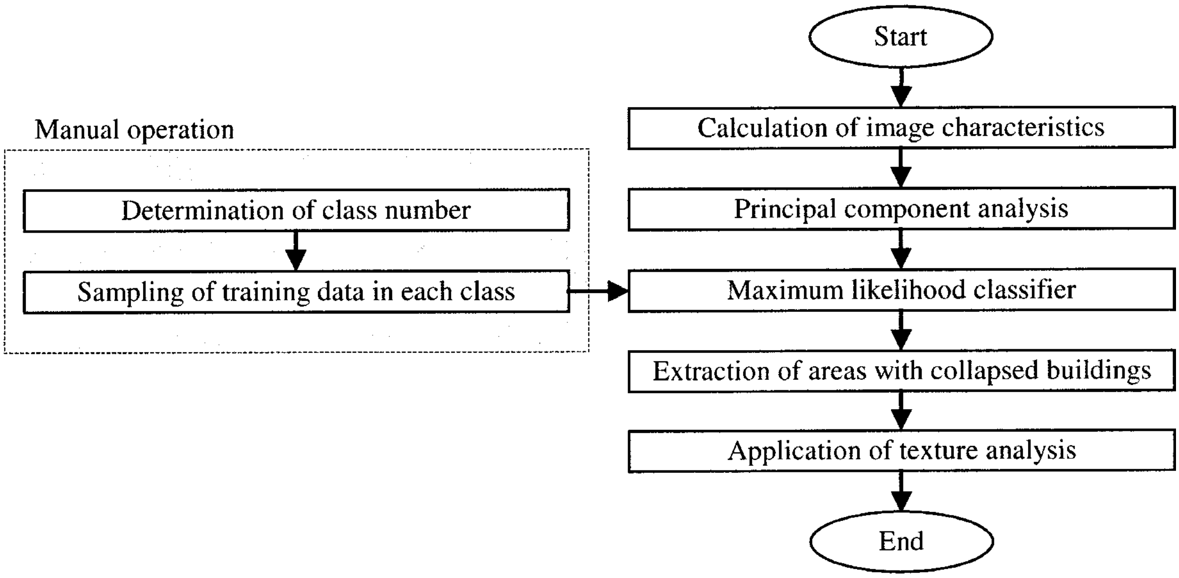

Figure 1. Flowchart of the method proposed in this study.

2 METHODOLOGY

2.1 *Previous method*

The steps of the automated detection method proposed by Hasegawa et al. (2000b) and applied by Mitomi et al. (2000) were as follows.

- Some training data were selected from typical damaged and undamaged areas in an image.
- Characteristics of the training data, such as hue, saturation, brightness, edge intensity and variance of edge intensity, were analyzed.
- Threshold values were decided from these characteristics for some damaged buildings.
- Pixels were extracted in combination with these threshold values.
- The local density of the selected pixels in the training data was calculated by a texture analysis.
- The areas of building damage were estimated using the threshold value for the texture analysis.

Selection of the training data and determining some threshold values for the characteristics and the texture analysis had to be empirically decided in this method because these values had to be changed depending on factors such as built environment and the influence of sunshine. In this study, we performed the method using the maximum likelihood classifier, which does not require the selection of training data to buildings of similar size and the determination of some threshold values.

2.2 *Application of maximum likelihood classifier*

Figure 1 shows the flowchart for this method. After a linear conversion, rationing and HSI transformation were performed on each input image, the characteristics of damage to wooden buildings were defined based on hue, saturation, brightness, edge intensity and variance of edge intensity. Color indices were not averaged by 7 x 7 pixels as done in the previous studies, because features of each input image should be maximally reflected. The edge intensity was calculated by a general gradient filter with a 3 x 3 pixel window. The variances in the edge intensity were evaluated for the area of 7 x 7 pixels.

The maximum likelihood classifier is one of the most popular classification methods in remote sensing, in which a pixel with the maximum likelihood is classified into the corresponding class. For mathematical reasons, a multivariate normal distribution is employed as the probability density

Kobe HDTV image (Nishinomiya)

Turkey television image (Golcuk)

Taiwan HDTV image (Chungalio)

Figure 2. Images used in this study.

function. In the case of normal distributions, the likelihood can be expressed as follows (Japan Association on Remote Sensing 1996).

$$Lci(x) = \frac{1}{(2\pi)^{k/2} |\ Vi\ |^{1/2}} \exp\left[-\frac{1}{2} \left(x - \overline{xi} \right)^t Vi^{-1} \left(x - \overline{xi} \right) \right]$$

where $Lci(x)$ = the likelihood of x belonging to class i; k = the number of image characteristics; x = the image data of k; $\overline{xi}$ = the mean vector of class i; Vi = the variance-covariance matrix of class i.

Most of the pixel values in the characteristic images of edge elements were close to zero, in particular, those of the roof and outside wall, whose color variations were much less than those of other objects, were almost zero. The maximum likelihood method cannot be applied if a determinant of the variance-covariance matrix derived from some training data becomes zero and an inverse of its matrix does not exist. For these reasons, the principal component analysis was introduced before the classification applying the maximum likelihood method. On the other hand, the number of classes and training data must be decided manually. However, the number of classes could be established again, if the result was not correct, by comparing the classification result with the actual situation. Thus, selection of training data does not have any constraints in order to attempt the principal component analysis. The class labeled as collapsed buildings refers to areas with building damage. Finally, the texture analysis, which is a spatial filtering technique, was attempted. Hence, it might be possible for us to extract areas with building damage automatically and rapidly, as we do not need to select training data depending on the size of a building and to estimate the threshold values for each image, as required in the previous studies empirically.

Table 1. Result of the principal component analysis for each input image

characteristics	1st	2nd	3rd	4th	5th
Kobe HDTV image					
eigenvalue	4581.3	2613.8	1312.6	834.05	241.49
eigenvector					
- hue	0.7891	-0.5889	0.1438	-0.0957	0.0257
- saturation	-0.1655	-0.3277	0.1867	0.9059	-0.0988
- brightness	0.5905	0.6785	-0.1912	0.3832	-0.0871
- edge intensity	0.0231	0.2476	0.8723	-0.1296	-0.4005
- variance of edge intensity	0.0266	0.1556	0.3833	0.0809	0.9064
variance (%)	47.806	27.274	13.697	8.703	2.520
cumulative variance (%)	47.806	75.080	88.777	97.480	100.000
Turkey television image					
eigenvalue	4226.0	1974.6	1038.5	862.75	237.61
eigenvector					
- hue	0.9617	-0.1469	0.2305	0.0186	-0.0017
- saturation	-0.2663	-0.6203	0.6956	0.2439	-0.0317
- brightness	-0.0501	0.7117	0.6770	-0.1787	-0.0264
- edge intensity	0.0352	0.2201	-0.0684	0.7063	-0.6684
- variance of edge intensity	0.0207	0.1965	-0.0072	0.6398	0.7427
variance (%)	50.675	23.678	12.452	10.346	2.849
cumulative variance (%)	50.675	74.353	86.805	97.151	100.000
Taiwan HDTV image					
eigenvalue	5898.8	2922.1	1302.9	388.19	96.856
eigenvector					
- hue	0.9345	0.3525	0.0482	0.0115	-0.0001
- saturation	0.1832	-0.5934	0.7833	0.0203	-0.0185
- brightness	-0.3033	0.7215	0.6184	-0.0623	-0.0347
- edge intensity	-0.0259	0.0397	0.0020	0.8749	-0.4820
- variance of edge intensity	-0.0223	0.0380	0.0422	0.4798	0.8753
variance (%)	55.603	27.544	12.281	3.659	0.913
cumulative variance (%)	55.603	83.147	95.428	99.087	100.000

3 EXTRACTION OF BUILDING DAMAGE AREAS

3.1 *Characteristics of images used in this study*

The Kobe, the Kocaeli, Turkey and the Chi-Chi, Taiwan earthquakes occurred on January 17, 1995, August 17, 1999 and September 21, 1999, respectively. Aerial imaging of areas damaged by the Kobe earthquake was started shortly after the event by the Japan Broadcasting Corporation (NHK). The Japanese Geotechnical Society took images of stricken areas a few weeks after the Turkey earthquake using a digital video camera from a helicopter. Two and four days after the Taiwan earthquake, NHK obtained images of severely damaged areas using a HDTV camera from a helicopter. In this study, we used images taken at Nishinomiya after the Kobe, Golcuk after the Kocaeli, Turkey, and Chungliao after the Chi-Chi, Taiwan earthquakes, which had suffered severe earthquake damage. These images are shown in Figure 2. Table 1 shows the results of the principal component analysis to each input image. Hue was the most influential characteristic of the five factors used for automatic detection of building damage. The cumulative variance from the first to the third principal component was more than about 90% in all input images, but the edge intensity and its variance make almost no contribution to the images. Some training data were determined as a

Table 2. Lists of items and extraction ratios in training data selected for five 10 x 10 pixels

Class	Characteristics of training data	Dr (%)	Dr' (%)
Kobe HDTV image			
Class-1	Debris of collapsed wooden buildings	65.4	65.4
Class-2	Severely damaged buildings with roof and wall	44.0	14.0
Class-3	Wall of undamaged low-rise wooden buildings	85.6	6.2
Class-4	Roof of undamaged low-rise wooden buildings	42.4	3.4
Class-5	Big roof of a gymnasium	92.6	0.0
Class-6	Blue sheets covering damaged wooden buildings	98.0	0.0
Class-7	Railways	94.0	0.6
Class-8	Road and parking lot made of asphalt	84.4	2.4
Class-9	School ground	90.2	8.0
Turkey television image			
Class-1	Debris of collapsed wooden buildings (brown)	59.4	59.4
Class-2	Severely damaged buildings (gray)	66.6	7.4
Class-3	Sound outside wall of undamaged buildings (sunny side)	93.0	10.0
Class-4	Sound outside wall including some windows	38.4	2.0
Class-5	Sound outside wall of undamaged buildings (shaded side)	41.0	2.4
Class-6	Roof of undamaged buildings (sunny side)	94.4	0.2
Class-7	Roof of undamaged buildings (shaded side)	74.8	3.0
Class-8	Road made of asphalt (sunny side)	89.4	10.4
Class-9	Road made of asphalt (shaded side)	94.4	0.4
Class-10	Seawater	89.8	4.8
Taiwan HDTV image			
Class-1	Debris of collapsed wooden buildings	79.2	79.2
Class-2	Severely damaged buildings with roof and wall	53.6	9.8
Class-3	Sound outside wall of undamaged buildings (white)	95.0	0.0
Class-4	Sound outside wall of undamaged buildings (gray)	76.4	2.8
Class-5	Roof of undamaged buildings (red)	94.6	0.0
Class-6	Roof of undamaged buildings (various colors)	67.4	1.0
Class-7	Roof of undamaged buildings (gray)	93.8	0.0
Class-8	Vegetation	96.0	0.0
Class-9	Boundary between sunny and shaded sides	74.2	7.2

class of classification from each image. Five 10 x 10 pixel windows, which were much smaller than subjects such as one building were manually sampled as training data in the same class. The classes and training data finally determined by this study are shown in Table 2. The maximum likelihood method was performed on nine classes in the Kobe and the Taiwan HDTV images. In the Turkey television image, the method was applied to ten classes. In all of the input images, the area including collapsed buildings was allocated to class-1.

3.2 *Extraction based on maximum likelihood classifier*

We defined an extraction ratio in each set of training data as an index of the extraction accuracy in each class for the maximum likelihood classifier.

$$Dr(i) = \frac{Dpx(i)}{Tpx(i)}$$

where $Dr(i)$ = the extraction ratio in each set of training data of class i; $Dpx(i)$ = the number of pixels classified as class i in each set of training data for class i; $Tpx(i)$ = the total number of pixels in each set of training data for class i. Table 2 also shows lists of extraction ratios obtained in this study. Most of the classes indicate high extraction ratios. Class-1 representing debris of collapsed

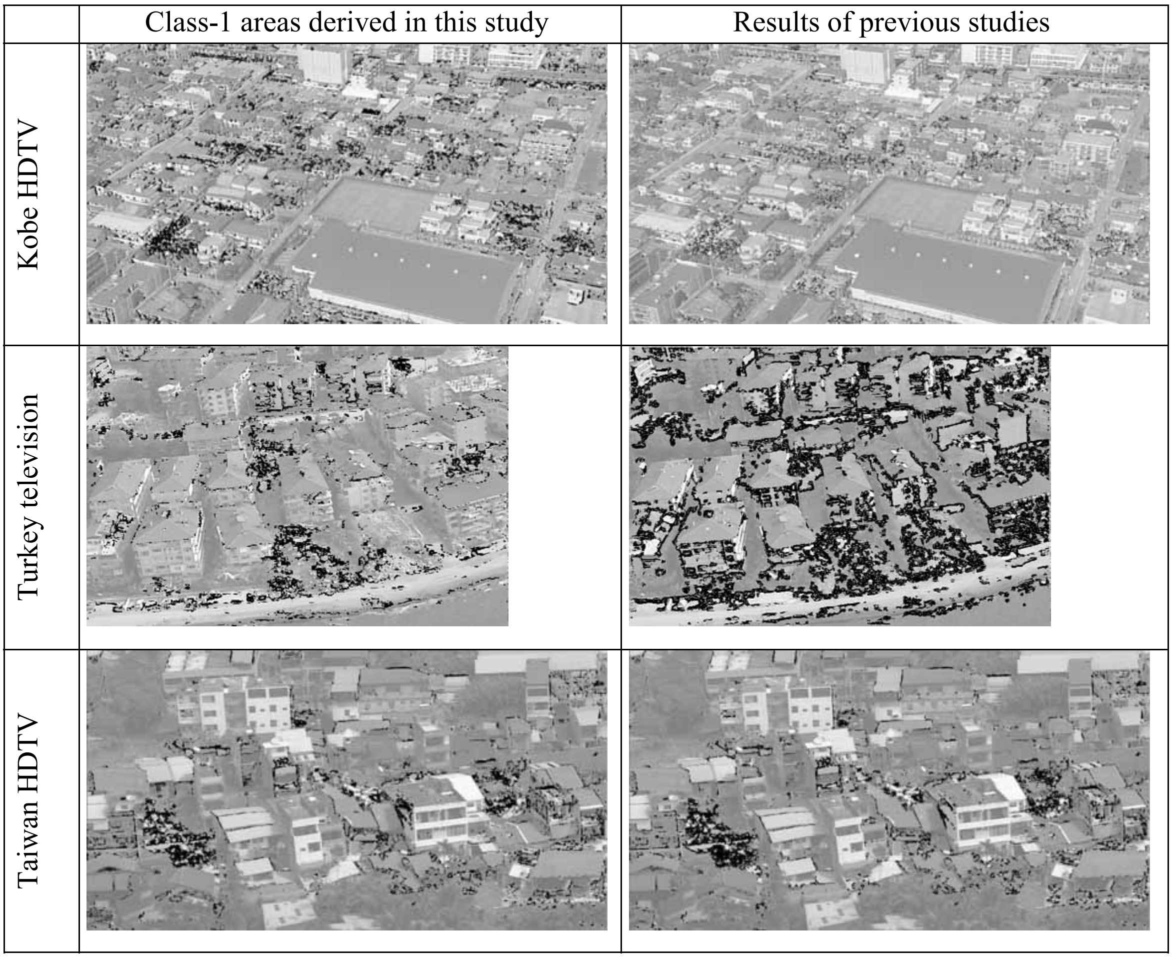

Figure 3. Comparison of the results of application of the maximum likelihood classifier and those by previous studies

buildings had a *Dr* value ranging from 60 to 80%. However, some classes had a low ratio because of misreading, since a pixel should be assigned to some class according to the maximum likelihood classifier. The distribution of class-1 by the maximum likelihood method and the results of the previous studies are shown in Figure 3. The results of this study seem to be clearer than those of the previous studies and are in good agreement with the actual situation. However, in the Turkey image, parts of class-1 were misread as class-2 because characteristics of class-1 were similar to those of class-2, and the classification of class-1 to class-2 was analogous to that of the previous study.

Using the equation for *Dr*, we derived *Dr'* as shown in Table 2, which is the ratio of the number of pixels classified as class-1 in each training data for class *i* against *Tpx*(*i*). In the previous study, extraction ratios of training data for collapsed buildings were about 25% in the Kobe, and 57% in the Turkey and Taiwan earthquakes, respectively. Therefore, the result based on this method had a better extraction ratio than that of the previous studies.

3.3 *Application of texture analysis*

A spatial filtering operation may be necessary to decrease surplus pixels and make areas with building damage easy to understand. In the previous study, the local density of the selected pixels was calculated by a texture analysis. In the Kobe HDTV image, 31 x 31 to 63 to 63 pixel windows were selected to be proportional to the image scale, depending on the location of the area. The pixel

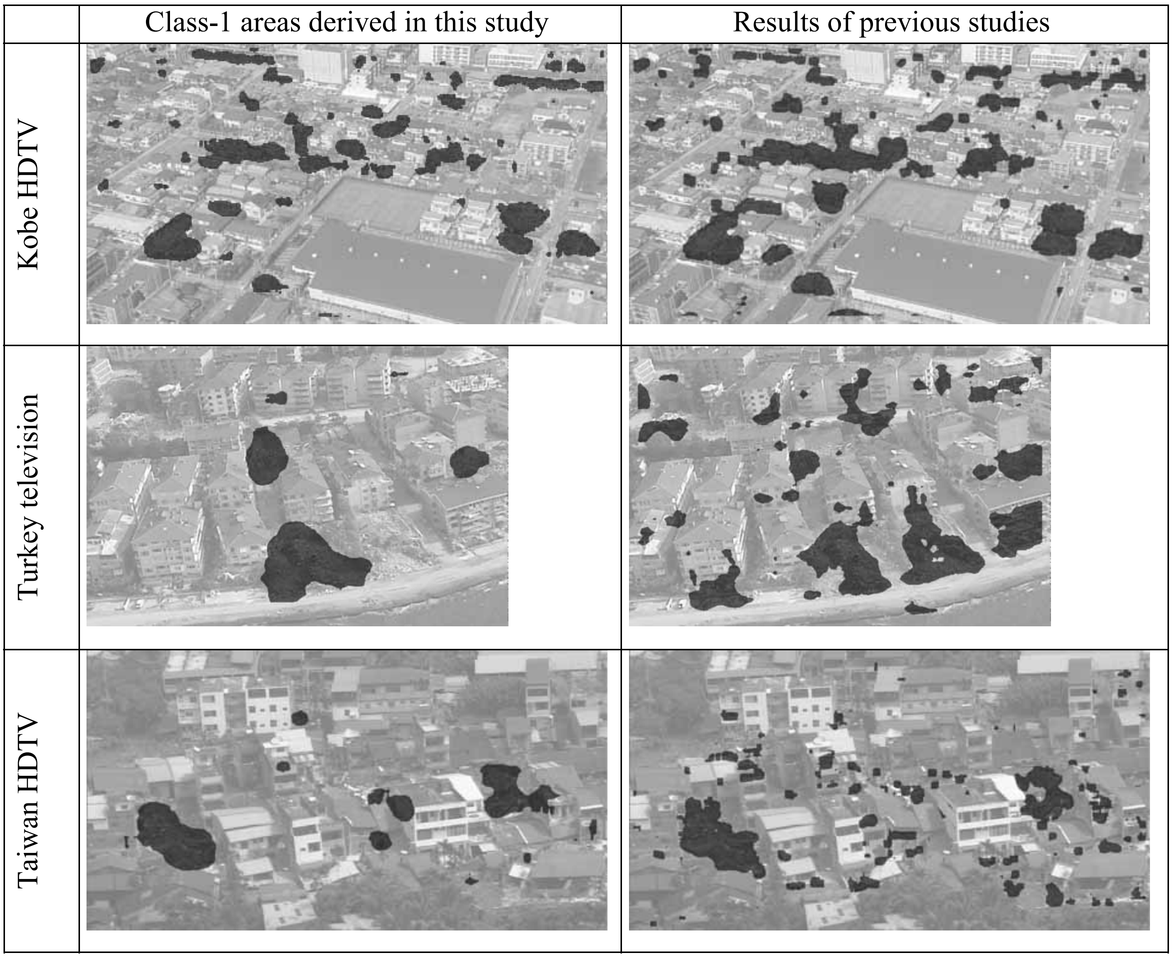

Figure 4. Comparison of the results of application of texture analysis and those by previous studies.

blocks whose density values were smaller than 14%, and larger than or equal to 14% were assigned as belonging to undamaged and collapsed buildings, respectively. A 31 x 31 pixel window as the minimum size applied to the Kobe image was used in the Turkey and Taiwan images, then, threshold values for the texture analysis were set to 43% and 30%, respectively.

In order to detect areas with building damage, the window size and threshold value for the texture analysis must be established in advance. As the window size corresponding to one building generally depended on factors such as the resolution of the image and built environment, each window size was decided based on the same method as for the Kobe image. It was changed from 57 x 57 to 83 x 83 pixels for the Turkey image, and set at a constant of 83 x 83 pixels for the Taiwan image. The threshold value between damaged and undamaged building areas was tentatively considered as 20% in all images. Figure 4 represents preliminary results from this study and from the previous studies. It is interesting that the distribution of areas with building damage in this study was in good agreement with the actual areas with building damage in spite of applying a common threshold value, 20%, in all images. We can hence obtain a good distribution of areas with building damage for every image using a constant threshold value for texture analysis, if we determine the window size to correspond to one building for every image.

4 CONCLUSIONS

An automated method to detect areas with building damage based on the maximum likelihood method was devised in order to further develop the method proposed in the previous studies. Hue, saturation, brightness, edge intensity and variance of edge intensity were used as image characteristics to determine the difference between damaged and undamaged building areas. Pixels representing areas with building debris could be relatively well grouped together. The principal component analysis was carried out in order to avoid that a determinant of the variance-covariance matrix derived from some training data becomes zero and that an inverse of its matrix cannot be obtained. Due to this operation, we could select some training data without any constraints. The number of classification schemes was nine or ten, and five 10 x 10 pixels were selected as training data. In the method proposed in this study, we could rapidly obtain a good agreement with the actual distribution for areas with building damage based on automated classification using a maximum likelihood classifier, if we appropriately decide the number of classes, and select some training data and a window size for the texture analysis. Hereafter, we intend to perform a further study to develop and establish a general method of automatic damage detection of buildings.

ACKNOWLEDGMENTS

The HDTV images taken after the Kobe and Taiwan earthquakes were provided by the Japan Broadcasting Corporation. The digital video images taken in the Turkey earthquakes were provided by Dr. N. Yoshida of Sato Kogyo Co., Ltd.

REFERENCES

Hasegawa, H., Yamazaki, F., Matsuoka, M. & Sekimoto, I. 2000a. Extraction of building damage due to earthquakes using aerial television images. *Proceedings of the 12th world conference on earthquake engineering*: No.1722: CD-ROM.

Hasegawa, H., Aoki, H., Yamazaki, F., Matsuoka, M. & Sekimoto, I. 2000b. Automated detection of damaged buildings using aerial HDTV images. *Proceedings of the IEEE 2000 international geoscience and remote sensing symposium*: IEEE: CD-ROM.

Japan Association on Remote Sensing. 1996. Remote sensing note. *Japan Association on Remote Sensing*: 220-221. Tokyo: Japan Association on Remote Sensing.

Mitomi, H., Yamazaki, F. & Matsuoka, M. 2000. Automated detection of building damage due to recent earthquakes using aerial television images. *Proceedings of the 21st Asian conference on remote sensing*: 401-406.

Nemoto, M., Ando, M., Shibata, K. & Imai, Y. 2000. Attempt for estimation of earthquake damage using ALOS images simulated from aerial photographs. *Proceedings of the autumn conference of the Japan society of photogrammetry and remote sensing*: 139-142 (in Japanese).

Ogawa, N. & Yamazaki, F. 2000. Photo-interpretation of building damage due to earthquakes using aerial photographs. *Proceedings of the 12th world conference on earthquake engineering*: No.1906: CD-ROM.